Supplementary Material (ESI) for Chemical Communications

New Insights into the Aggregation of Silver Pyrazolides Using Sterically Hindered Bidentate Pyrazole Ligands

James J. Henkelis, Colin A. Kilner and Malcolm A. Halcrow*

School of Chemistry, University of Leeds, Woodhouse Lane, Leeds LS2 9JT, UK.
E-mail: m.a.halcrow@leeds.ac.uk

Electronic Supplementary Information

Synthetic Procedures and Characterisation Data for the Compounds in this Work.

Ligands HL^1 [1] and HL^2 [2] were prepared by the literature procedures, while all other reagents were purchased commercially and used as supplied. Reactions were performed under ambient conditions using undried AR-grade solvents. Mass spectrometry data are listed below, in Table S6.

Synthesis of Ag[L^1] (1). A mixture of HL^1 (0.30 g, 1.5 mmol) and $AgBF_4$ (0.29 g, 1.5 mmol) in MeOH (50 cm^3) was stirred at room temperature until all the solid had dissolved. $^nBu_4NOH$ (1.5 cm^3 of a 1.0 M solution in MeOH, 1.5 mmol) was then added with stirring, leading to the immediate formation of a gelatinous off-white precipitate. Stirring was continued at room temperature for 30 mins, then the mixture left to settle at –30°C overnight. The solid was collected by filtration, washed with MeOH and Et_2O, and dried *in vacuo*. The product is sparingly soluble, but mg amounts can be recrystallised from 1,2-$C_2H_4Cl_2$/Et_2O. Yield 0.40 g, 63 %. Found C, 46.6; H, 4.55; N, 13.3 %. Calcd for $[C_{12}H_{14}AgN_3]_n$ C, 46.8; H, 4.58; N 13.6 %. IR (nujol): 3050w, 2727w, 1593s, 1566m, 1523w, 1488s, 1396w, 1359m, 1328m, 1276w, 1245m, 1205m, 1195m, 1135m, 1106m, 1080m, 1069m, 1036m, 1001w, 979w, 876w, 792m, 765s, 739m, 687w, 628m cm^{-1}. ^1H NMR ($CDCl_3$): the spectrum is strongly broadened and shows two unique $[L^1]^-$ environments in an approximate 3:2 integral ratio. δ 1.35 (br s, 9H x 0.4, minor CCH_3), 1.54 (br s, 9H x 0.6, major CCH_3), 6.55 (br s, 1H x 0.4, minor pz H^4), 6.68 (br s, 1H x 0.6, major pz H^4), 7.07 (br s, 1H, major + minor py H^5), 7.64 (br s, 2H, major + minor py H^3 + H^4), 8.25 (br s, 1H x 0.4, minor py H^6), 8.44 (br s, 1H x 0.6, major py H^6). UV/vis (CH_2Cl_2): λ_{max}, nm (ε_{max}, 10^3 dm^3 mol^{-1} cm^{-1} per Ag[L^1] formula unit) 263 (8.1), 297 (7.5).

Synthesis of [$Ag_3Br(L^1)_2$] (2). Recrystallisation of **1** (0.30 g, 0.84 mmol) from pyridine/diethyl ether affords analytically pure colourless crystals of **2** over a period of 1 week. Addition of $^nBu_4NBr$ (0.14 g, 0.42 mmol) to the solution increased the rate of crystallisation, which was then complete in 48 hrs, but did not significantly affect the yield of the product. Solid **2** is only sparingly soluble, and its solutions in chlorinated solvents slowly precipitate AgBr over a period of hours. Yield 0.05 g, 22 %. Found C, 36.3; H, 3.50; N, 10.6 %. Calcd for $C_{24}H_{28}Ag_3BrN_6$ C, 35.9; H, 3.51; N 10.5 %. IR (nujol): 3133w, 3068m, 2714w, 1610w, 1593s, 1567m, 1527w, 1488m, 1397w, 1359m, 1322m, 1276m, 1245s, 1205m, 1193m, 1148m, 1133s, 1106m, 1082m, 1049m, 1034s, 1001m, 979m, 960w, 948w, 876m, 794m, 765s, 738m, 684m, 629m, 602w cm^{-1}. ^1H NMR ($CDCl_3$): δ 1.46 (br s, 18H, CCH_3), 6.63 (br s, 2H, pz H^4), 7.04 (br s, 2H, py H^5), 7.68 (br s, 4H, py H^3 + H^4), 8.14 (br s, 2H, py H^6). UV/vis (CH_2Cl_2): λ_{max}, nm (ε_{max}, 10^3 dm^3 mol^{-1} cm^{-1} per [$Ag_3Br(L^1)_2$] formula unit) 264 (23.5), 297 (20.1).

Synthesis of [$Ag_{10}(L^1)_8$]Cl_2 (3). Addition of $^nBu_4NCl$ (0.12 g, 0.42 mmol) to a pyridine solution of **1** (0.30 g, 0.84 mmol) yields a pale yellow solution and a black precipitate, which was removed by filtration. Diffusion of diethyl ether vapour into the filtrate initially gives an oil, which partially crystallises to colourless plates of **3** over a period of days. Unfortunately, the remaining oil contaminating the crystals prevented us from obtaining a good microanalysis of the material. While **3** is sparingly soluble in most organic solvents, its dissolution is accompanied by formation of an AgCl precipitate. The presence of chloride in the product is also supported by mass spectrometry data (Table S6, see below). IR (nujol): 3168w, 3114w, 2726w, 1600w, 1589s, 1563m, 1523w, 1483s, 1360m, 1324m, 1286w, 1273w, 1243m, 1207m, 1194w, 1168w, 1148s, 1128m, 1103m, 1078m, 1055w, 1044w, 1024s, 994w, 976m, 964w, 934w, 880s, 794s, 763s, 740m, 689w, 622m cm^{-1}. ^1H NMR (CD_3CN): δ 1.42 (s, 9H, CCH_3), 6.66 (s, 2H, pz H^4), 7.18 (br s, 1H, py H^5), 7.70 (d, 9.0 Hz, 1H, Py H^3), 7.72 (pseudo-t, 7.8 Hz, 1H, py H^4), 8.42 (br d, 4.8 Hz, 1H, py H^6). Since an AgCl precipitate was removed from the CD_3CN solution before the spectrum was acquired, this is unlikely to be the true NMR spectrum of **3**.

Synthesis of $[Ag_4(L^2)_4]\cdot x H_2O$ ($4\cdot x H_2O$; $x \approx 3$). Reaction of HL^2 (0.38 g, 1.5 mmol), $AgBF_4$ (0.29 g, 1.5 mmol) and $^nBu_4NOH$ (1.5 cm^3 of a 1.0 M solution in MeOH, 1.5 mmol) in MeOH (50 cm^3) at room temperature yields a pale green solution, which quickly deposited a small amount of precipitate that was removed by filtration. The filtered solution was stored at room temperature for 3 days, slowly depositing the product as an off-white crystalline solid. The compound was isolated by filtration, washed with MeOH and dried *in vacuo*. Yield 0.15 g, 28 %. Found C, 51.5; H, 4.30; N, 11.1 %. Calcd for $C_{64}H_{64}Ag_4N_{12}\cdot 3H_2O$ C, 51.7; H, 4.75; N, 11.3 %. IR (nujol): 3049w, 2726w, 1619m, 1585m, 1555m, 1498w, 1422w, 1413w, 1362w, 1330s, 1312w, 1266w, 1240m, 1220w, 1206w, 1141m, 1054s, 1033s, 1019m, 956m, 875m, 822s, 804m, 789w, 753m, 674s, 663w cm^{-1}. ^{1}H NMR ($CDCl_3$): δ 1.35 (s, 48H, CCH_3), 1.6 (v br, 6H, H_2O), 6.70 (br s, 4H, pz H^4), 7.42 (br s, 4H, iqn H^4), 7.64 (pseudo-t, 9.0 Hz, 8H, iqn H^6 + H^7), 7.79 (br s, 4H, iqn H^5), 8.09 (br s, 4H, iqn H^8), 8.58 (d, 7.4 Hz, 4H, iqn H^3). UV/vis (CH_2Cl_2): λ_{max}, nm (ε_{max}, 10^3 dm^3 mol^{-1} cm^{-1} per $Ag_4[L^2]_4$ formula unit) 293 (sh), 300 (29.1), 337 (31.4).

Other measurements. Elemental microanalyses were performed by the University of Leeds School of Chemistry microanalytical service. IR spectra were run using a Nicolet Paragon 1000 spectrometer, using nujol mull samples held between NaCl windows. Electrospray mass spectra were obtained on a Waters ZQ4000 spectrometer, from CH_2Cl_2 (**1**, **2** and **4**) or MeCN (**3**) feed solutions. ^{1}H NMR spectra employed a Bruker DPX300 spectrometer operating at 300.2 MHz. UV/vis spectra were obtained in 1 cm quartz cells with a PerkinElmer Lambda900 spectrophotometer.

Table S1 Experimental data for the single crystal structure determinations in this work.

	α-$[Ag_3(\mu\text{-}Br)(\mu\text{-}L^1)_2]$ (α-**2**)	β-$[Ag_3(\mu\text{-}Br)(\mu\text{-}L^1)_2]$ (β-**2**)	$[Ag_{10}(\mu\text{-}L^1)_8]Cl_2$ (**3**)	$[Ag_4(\mu\text{-}L^2)_4]\cdot xH_2O$ (**4**$\cdot xH_2O$; x = 2.7)
Molecular formula	$C_{24}H_{28}Ag_3BrN_6$	$C_{24}H_{28}Ag_3BrN_6$	$C_{96}H_{112}Ag_{10}Cl_2N_{24}$	$C_{64}H_{64}Ag_4N_{12}$
M_r	804.04	804.04	2751.70	1432.75
Crystal class	Triclinic	Monoclinic	Monoclinic	Orthorhombic
Space group	$P\bar{1}$	$P2_1/c$	$C2/c$	$Fdd2$
a (Å)	9.6895(12)	12.9535(13)	25.170(2)	18.6771(12)
b (Å)	11.8611(14)	9.6805(9)	17.8880(14)	44.784(3)
c (Å)	11.9531(13)	21.741(2)	24.0804(18)	17.1502(11)
α (°)	100.553(6)	–	–	–
β (°)	92.229(6)	99.199(5)	100.925(4)	–
γ (°)	91.219(6)	–	–	–
V (Å^3)	1348.9(3)	2691.2(5)	10645.3(15)	14344.9(15)
Z	2	4	4	8
μ (Mo-K$_\alpha$) (mm^{-1})	3.661	3.661	1.851	1.118
T (K)	150(2)	150(2)	150(2)	150(2)
Measured reflections	35404	74513	116871	49319
Independent reflections	8185	6763	12807	9369
R_{int}	0.047	0.075	0.065	0.044
R_1 [$I > 2\sigma(I)$][a]	0.047	0.020	0.084	0.038
wR_2 (all data)[b]	0.191	0.051	0.286	0.119
Goodness of fit	1.062	1.104	1.115	1.045
Flack parameter	–	–	–	–0.02(3)

[a] $R = \Sigma[\,|F_o| - |F_c|\,] / \Sigma|F_o|$ [b] $wR = [\Sigma w(F_o^2 - F_c^2) \;/\; \Sigma wF_o^4]^{1/2}$

Experimental Procedures for the Crystal Structure Determinations in this Work
All diffraction data were collected using a Bruker X8 Apex diffractometer, with graphite-monochromated Mo-K_α radiation (λ = 0.71073 Å) generated by a rotating anode. The diffractometer was fitted with an Oxford Cryostream low temperature device. The structures were solved by direct methods (*SHELXS97*[3]), and developed by cycles of full least-squares refinement on F^2 and difference Fourier syntheses (*SHELXL97*[3]). All crystallographic Figures were produced using *XSEED*,[4] which incorporates *POVRAY*.[5] Experimental data for the crystal structures are listed in Table S1.

Crystallographic refinement of the two polymorphs of [Ag$_3$(μ-Br)(μ-L^1)$_2$] (2). The two polymorphs of [Ag$_3$(μ-Br)(μ-L^1)$_2$] co-crystallise upon slow diffusion of diethyl ether vapour into a solution of [AgL^1] in pyridine. Experimental details for the structure determinations are given in Table S2. The asymmetric units of both polymorphs contain discrete [Ag$_3$(μ-Br)(μ-L^1)$_2$] molecules, which associate into centrosymmetric dimers through weak argentophilic and second-sphere Ag...Br interactions.

In both polymorphs the *tert*butyl group C(31)-C(34) is disordered over two sites labelled 'A' and 'B'. In the α-form these four disordered atoms were modelled with a refined occupancy ratio of 0.68:0.32, while in the β-structure the same groups had a refined occupancy of 0.69:0.31, and were modelled with a common wholly occupied quaternary C atom C(31). The fixed restraints C–C = 1.52(2) and 1,3-C...C = 2.48(2) Å were applied to the disordered *tert*butyl groups in both structures. All non-H atoms except for the minor tert-butyl disorder site were refined anisotropically in both structures, and all H atoms were placed in calculated positions and refined using a riding model. The final refinement of the α-structure showed a highest residual Fourier peak of +1.4 e.Å^{-3} 0.4 Å from Ag(3), and a largest Fourier trough of –4.8 e.Å^{-3} that is associated with Br(4). There are no noteworthy Fourier peaks or troughs in the final Fourier map from the β-structure refinement. CCDC 806534 (α-**2**) and 806535 (β-**2**).

Crystallographic refinement of [Ag$_{10}$(μ-L^1)$_8$]Cl$_2$ (3). The asymmetric unit contains half a cluster molecule spanning the crystallographic C_2 axis at 0, y, ¼, and a disordered region of electron density occupying a void in the lattice that spans the crystallographic inversion centre at ¼, ¼, ½. Each void was presumed to contain two anions on charge balancing grounds, which were likely to be either BF_4^- or Cl^- based on the contents of the reaction mixture. A *SQUEEZE*[6] analysis of the isotropically refined model found four voids of 248 Å^3 per unit cell, containing a total of 152 electrons. That equates to 38 electrons per void, or 19 electrons per asymmetric unit. Thus, there appears to be one disordered chloride ion (18 electrons) in the asymmetric unit. The original dataset, rather than the *SQUEEZE*d one, was used for the final refinement cycles. Seven Fourier peaks in the disordered region were located, which were each refined as 0.1 of a Cl atom. The remaining 0.3 of a Cl atom could not be located in the Fourier map, but was included in the density and F(000) calculations. The presence of chloride in the crystal is also supported by mass spectrometry data (see below), and by the formation of an AgCl precipitate when the material is redissolved in organic solvents.

Three of the four unique tertbutyl groups in the model are disordered over two sites, that were each modelled with a 0.6:0.4 occupancy ratio. Disorder sites were refined for the complete *tert*butyl fragments C(17)-C(20) and C(62)-C(65), but the third disordered *tert*butyl moiety was refined with partial methyl groups C(33)-C(35) only, which shared a common wholly-occupied *ipso*-C atom C(32). The fixed restraints C–C = 1.52(2) and 1,3-C...C = 2.48(2) Å were applied to the disordered residues. All fully occupied non-H atoms were refined anisotropically, and H atoms were placed in calculated positions and refined using a riding model. There are several residual Fourier peaks between 2.0 and 3.9 e.Å^{-3} in the final model, all of them 1.0-1.3 Å from an Ag atom. CCDC 806536.

Crystallographic refinement of $[Ag_4(\mu\text{-}L^2)_4]\cdot x H_2O$ ($4\cdot x H_2O$). The asymmetric unit contains half a complex molecule, with Ag(2) and Ag(3) lying on the crystallographic C_2 axis ¼, ¼, *z*, and a series of weak Fourier peaks that are not bonded to any other atom and were modelled as partial water molecules. The refined occupancies of these partial water sites sum to 1.35, or 2.70 per formula unit. The presence of *ca*. 3 molar equivalents of water in the bulk material is supported by elemental microanalysis and by ^{1}H NMR.

One of the two unique *tert*butyl groups in the model, C(38)-C(41), is disordered over two equally occupied sites labelled 'A' and 'B'. This was refined with the fixed restraints C–C = 1.52(2) and 1,3-C...C = 2.48(2) Å. All non-H atoms were refined anistropically, and C-bound H atoms were placed in calculated positions and refined using a riding model. The partial water H atoms were not located or refined, but were included in the density and *F*(000) calculations. CCDC 806537.

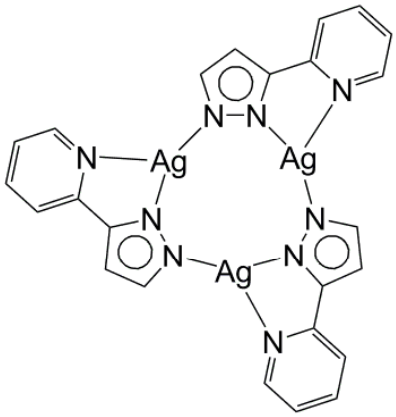

$[Ag_3(pz^{Py})_3]$[7]

This is the most common structure for coinage metal salts of monodentate, as well as chelating, pyrazolides.[8,9]

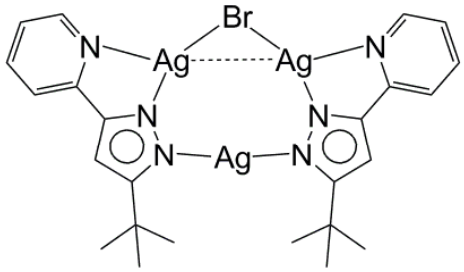

2

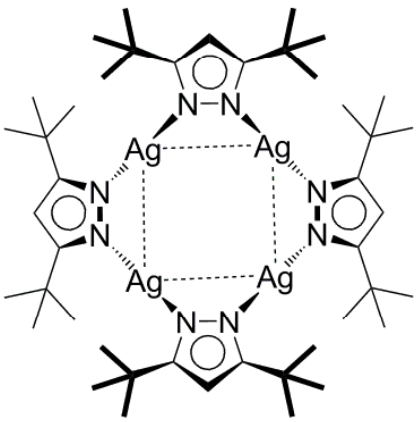

$[Ag_4(pz^{tBu2})_4]$[9,10]

Several copper(I) pyrazolides with bulky substituents also have this tetranuclear connectivity.[9,11]

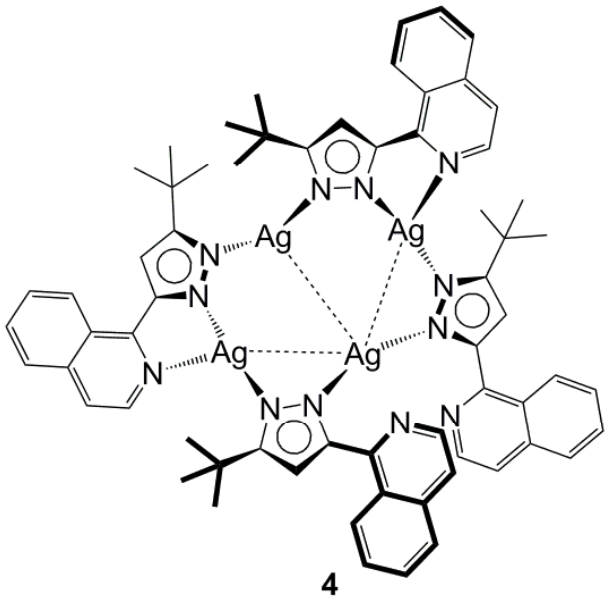

4

Scheme S1 Comparison of the connectivities of **2** and **4** with those in more conventional trinuclear and tetranuclear silver(I) pyrazolides. Argentophilic contacts of <3.5 Å are marked as dotted lines.

Table S2 Selected interatomic distances and angles in the two polymorphs of **2** (Å, °). See Fig. 1 of the main paper for the atom number scheme employed.

	α-form	β-form
Ag(1)–N(13)	2.119(5)	2.1496(18)
Ag(1)–N(28)	2.122(5)	2.1465(18)
Ag(2)–Br(4)	2.5452(9)	2.5611(4)
Ag(2)–N(5)	2.496(5)	2.5312(19)
Ag(2)–N(12)	2.210(5)	2.1919(19)
Ag(3)–Br(4)	2.5424(10)	2.5605(3)
Ag(3)–N(20)	2.524(5)	2.4674(19)
Ag(3)–N(27)	2.201(5)	2.1975(19)
Ag(1)...Ag(2)	3.6864(7)	3.6157(4)
Ag(1)...Ag(3)	3.7473(8)	3.7469(4)
Ag(2)...Ag(3)	3.0267(7)	2.9503(3)
N(13)–Ag(1)–N(28)	167.88(19)	169.87(7)
Br(4)–Ag(2)–N(5)	113.14(12)	108.45(5)
Br(4)–Ag(2)–N(12)	167.19(13)	166.28(5)
N(5)–Ag(1)–N(12)	72.07(17)	71.60(7)
Br(4)–Ag(3)–N(20)	115.43(12)	115.47(5)
Br(4)–Ag(3)–N(37)	163.34(13)	171.14(5)
N(20)–Ag(3)–N(27)	72.03(18)	73.15(7)

Table S3 Selected inter-cluster distances in the dimeric aggregates in the two polymorphs of **2** (Å). See Fig. 1 of the main paper for the atom number scheme employed. Symmetry codes: (i) –*x*, 2–*y*, 1–*z*; (ii) –*x*, 1–*y*, 1–*z*.

α-form		β-form	
Ag(1)–Br(4^{i})	3.2187(10)	Ag(1)–Br(4^{ii})	3.1938(4)
Ag(1)...Ag(2^{i})	3.4884(7)	Ag(1)...Ag(2^{ii})	4.2316(4)
Ag(1)...Ag(3^{i})	3.4385(8)	Ag(1)...Ag(3^{ii})	4.6565(4)
Ag(2)...Ag(3^{i})	3.4184(7)	Ag(2)...Ag(3^{ii})	3.0774(3)

Table S4 Metric parameters for *intra*- and *inter*-dimer π-π interactions in the two polymorphs of **2** (Fig. S2). See Fig. 1 of the main paper for the atom number scheme employed. Symmetry codes: (i) –*x*, 2–*y*, 1–*z*; (ii) –*x*, 1–*y*, 1–*z*; (v) 1–*x*, 2–*y*, 1–*z*; (vi) –*x*, –*y*, 1–*z*.

	Interplanar dihedral angle (°)	Interplanar distance (Å)	Centroid offset (Å)
α-form			
[N(5)-C(15)]...[N(20^{i})-C(30^{i})]	11.4(2)	3.50(2)	0.2
[N(5)-C(15)]...[N(5^{v})-C(15^{v})]	0	3.21(2)	1.9
β-form			
[N(5)-C(15)]...[N(20^{ii})-C(30^{ii})]	8.27(9)	3.314(10)	1.7
[N(20)-C(30)]...[N(20^{vi})-C(30^{vi})]	0	3.526(7)	2.3

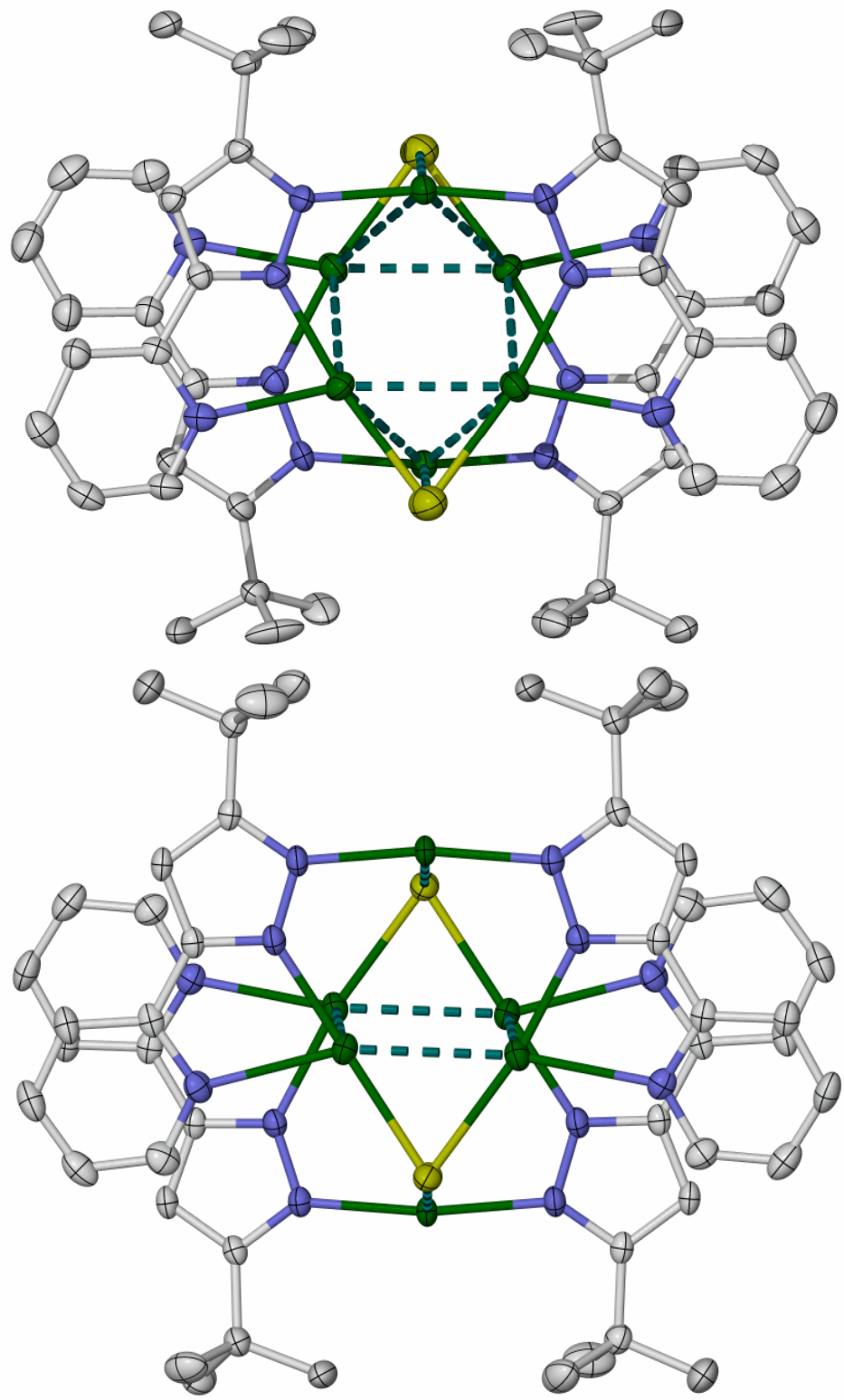

Fig S1 Views of the dimer-of-trimers in the α- (top) and β- (bottom) polymorphs of **2**. Only one orientation of the disordered tertbutyl group is shown, and H atoms have been omitted for clarity. All Ag...Ag and Ag...Br contacts of ≤3.5 Å are shown as dotted interactions. Alternative views are given in Fig. 2 of the main paper. Colour code: C, white; Ag, green; Br, yellow; N, blue.

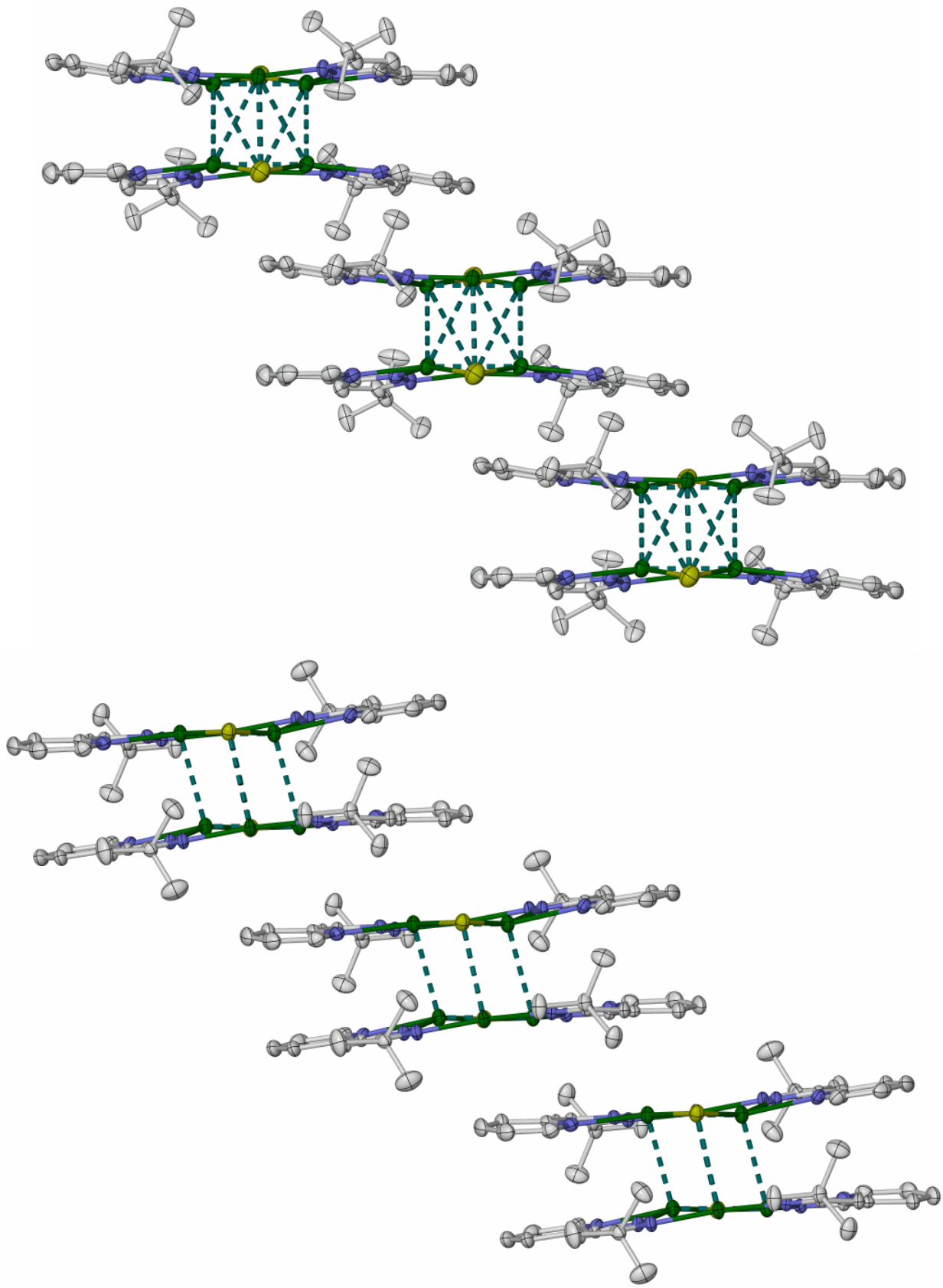

Fig S2 Partial packing diagrams of α- (top) and β- (bottom) **2**, showing the association of the supra-molecular dimers into 1D chains through π-π interactions (Table S4). The stacks run parallel to the (100) and (010) crystallographic vectors, respectively.

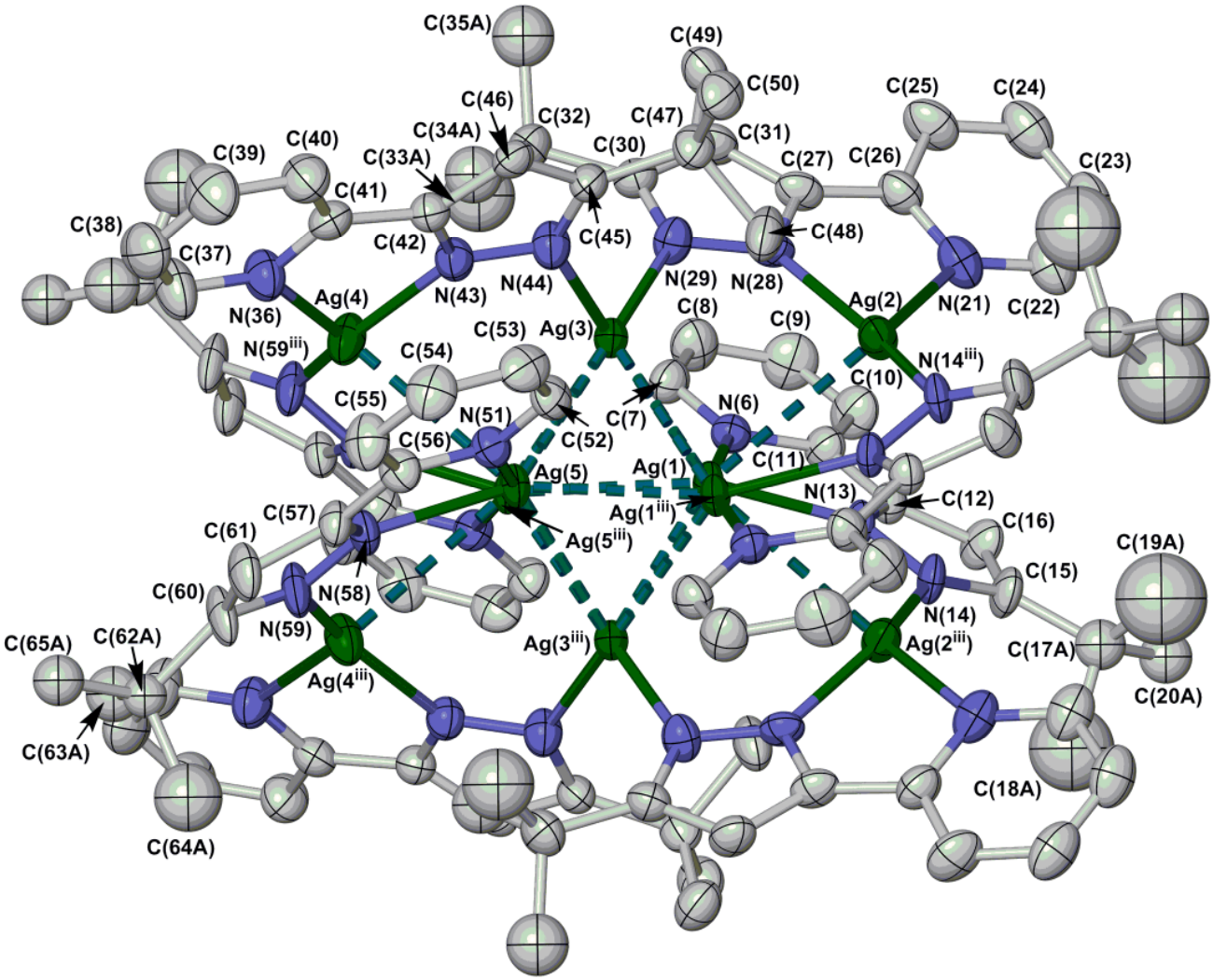

Fig S3 View of the $[Ag_8(\mu\text{-}L^1)_{10}]^{2+}$ dication in **3**, showing the full atom numbering scheme employed. Details as for Fig. S1. Symmetry code: (iii) *–x*, *y*, ½*–z*.

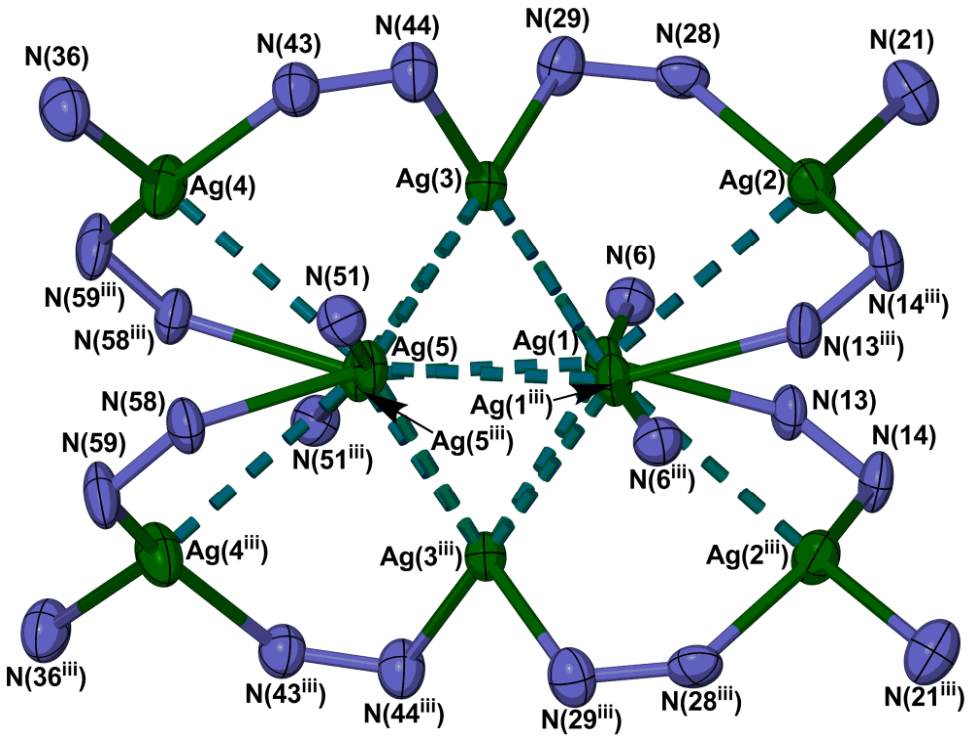

Fig S4 View of the silver/nitrogen core of the $[Ag_8(\mu\text{-}L^1)_{10}]^{2+}$ dication in **3**. The view is the same as in Fig. S2. Details as for Fig. S1. Symmetry code: (iii) *–x*, *y*, ½*–z*.

Table S5 Selected interatomic distances and angles in the structure of **3** (Å, °). See Figs. S3 and S4 for the atom number scheme employed. Symmetry code: (iii) *–x*, *y*, ½*–z*.

Ag(1)–N(6)	2.414(9)	Ag(1)...Ag(1^{iii})	2.7844(15)
Ag(1)–N(13)	2.234(8)	Ag(1)...Ag(2)	3.1380(12)
Ag(2)–N(14^{iii})	2.156(10)	Ag(1)...Ag(3)	2.7931(11)
Ag(2)–N(21)	2.625(12)	Ag(1)...Ag(3^{iii})	2.9012(11)
Ag(2)–N(28)	2.186(9)	Ag(1)...Ag(5^{iii})	2.7393(11)
Ag(3)–N(29)	2.272(10)	Ag(2)...Ag(2^{iii})	4.3012(18)
Ag(3)–N(44)	2.283(10)	Ag(2)...Ag(3)	3.7223(12)
Ag(4)–N(36)	2.621(11)	Ag(3)...Ag(4)	3.6939(12)
Ag(4)–N(43)	2.188(10)	Ag(3)...Ag(5)	2.8011(11)
Ag(4)–N(59^{iii})	2.157(11)	Ag(3)...Ag(5^{iii})	2.8807(11)
Ag(5)–N(51)	2.454(9)	Ag(4)...Ag(4^{iii})	4.3285(20)
Ag(5)–N(58)	2.229(9)	Ag(4)...Ag(5)	3.1218(13)
		Ag(5)...Ag(5^{iii})	2.7940(15)
N(6)–Ag(1)–N(13)	72.5(3)	N(36)–Ag(4)–N(43)	70.1(4)
N(14^{iii})–Ag(2)–N(21)	132.1(4)	N(36)–Ag(4)–N(59^{iii})	133.9(4)
N(14^{iii})–Ag(2)–N(28)	153.1(4)	N(43)–Ag(4)–N(59^{iii})	151.5(4)
N(21)–Ag(2)–N(28)	69.8(4)	N(51)–Ag(5)–N(58)	71.6(3)
N(29)–Ag(3)–N(44)	110.3(4)		

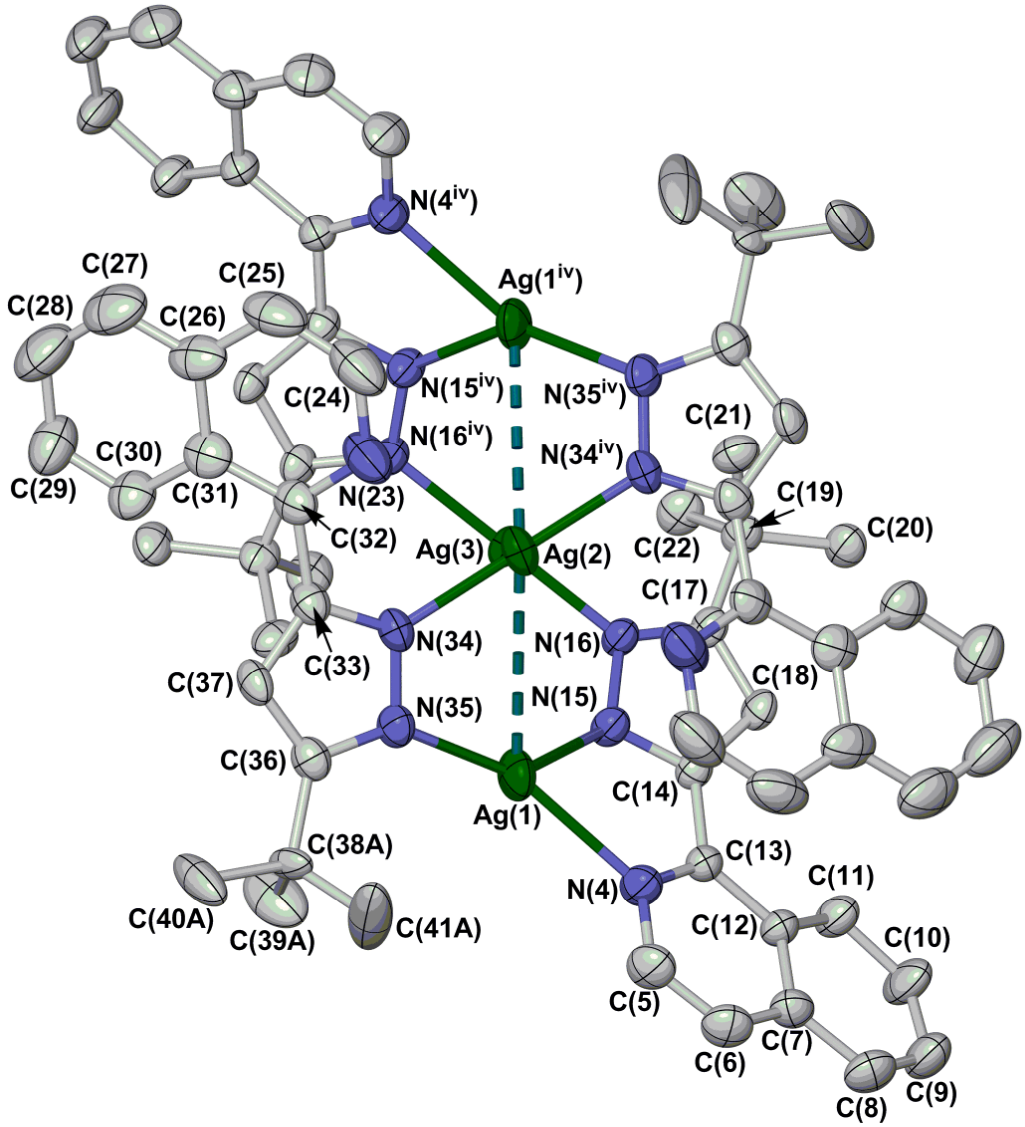

Fig S5 View of the $[Ag_4(\mu\text{-}L^2)_4]$ molecule in **4**·xH$_2$O, showing the full atom numbering scheme employed. The view is looking approximately down the crystallographic C_2 axis bisecting Ag(2) and Ag(3). Details as for Fig. S1. Colour code: C, white; Ag, green; N, blue. Symmetry code: (iv) ½–x, ½–y, z.

Table S6 Selected interatomic distances and angles in the structure of **4**·xH$_2$O (Å, °). See Fig. S5 for the atom number scheme employed. Symmetry code: (iv) ½–x, ½–y, z.

Ag(1)–N(4)	2.392(3)	Ag(3)–N(16)	2.096(3)
Ag(1)–N(15)	2.236(3)	Ag(1)...Ag(2)	3.3722(4)
Ag(1)–N(35)	2.143(3)	Ag(1)...Ag(3)	3.8410(5)
Ag(2)–N(34)	2.105(3)	Ag(2)...Ag(3)	3.0724(6)
N(4)–Ag(1)–N(15)	71.52(11)	N(34)–Ag(2)–N(34^{iv})	176.2(2)
N(4)–Ag(1)–N(35)	149.58(13)	N(16)–Ag(3)–N(16^{iv})	177.6(2)
N(15)–Ag(1)–N(35)	138.66(12)		

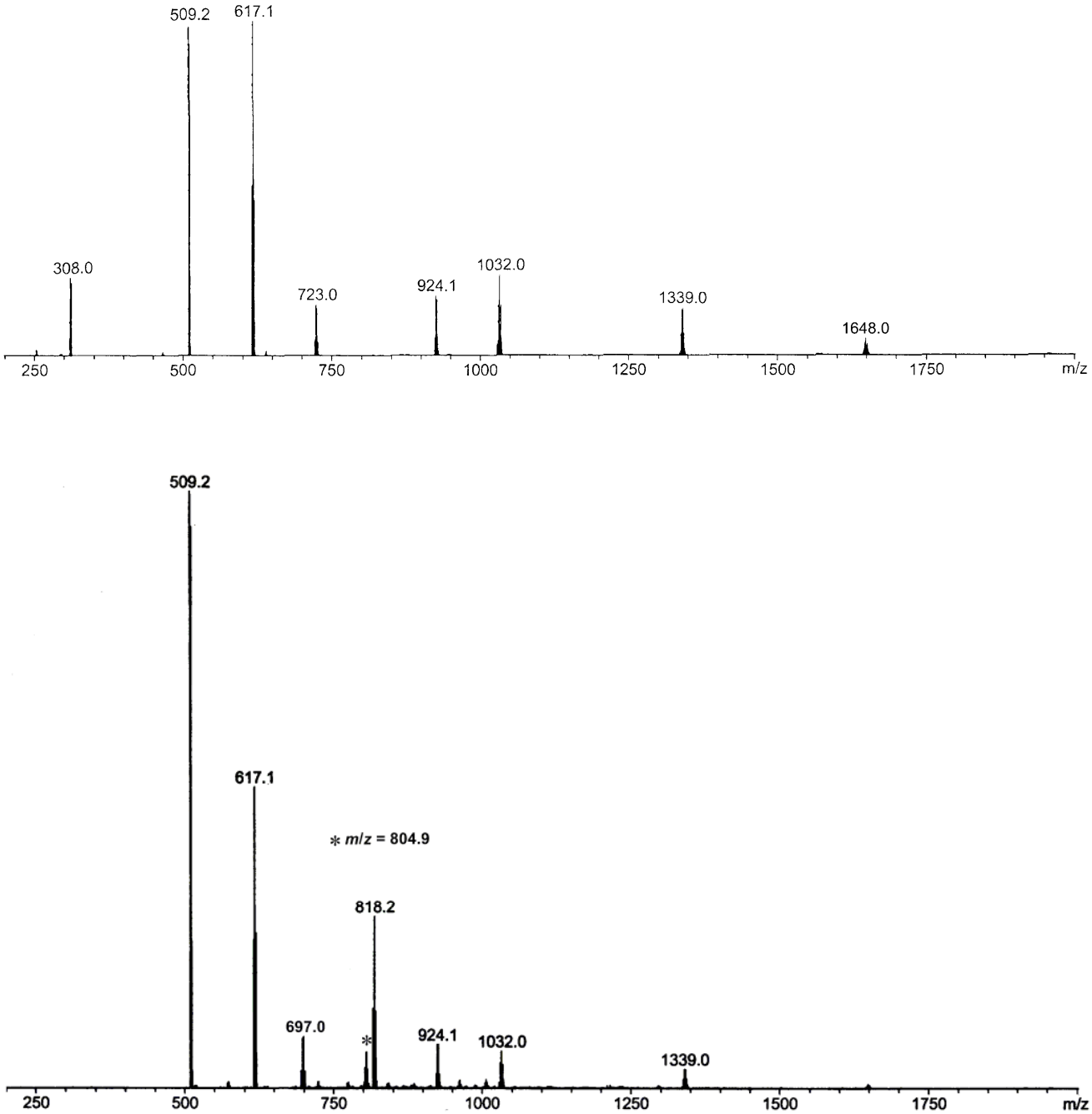

Fig S6 Electrospray mass spectra of **1** (top) and **2** (bottom) from CH_2Cl_2 solution. See Table S7 for the peak assignments. The starred peak at *m*/*z* = 804.9 corresponds to the intact, protonated molecular ion from compound **2**, $[Ag_3Br(L^1)(HL^1)]^+$.

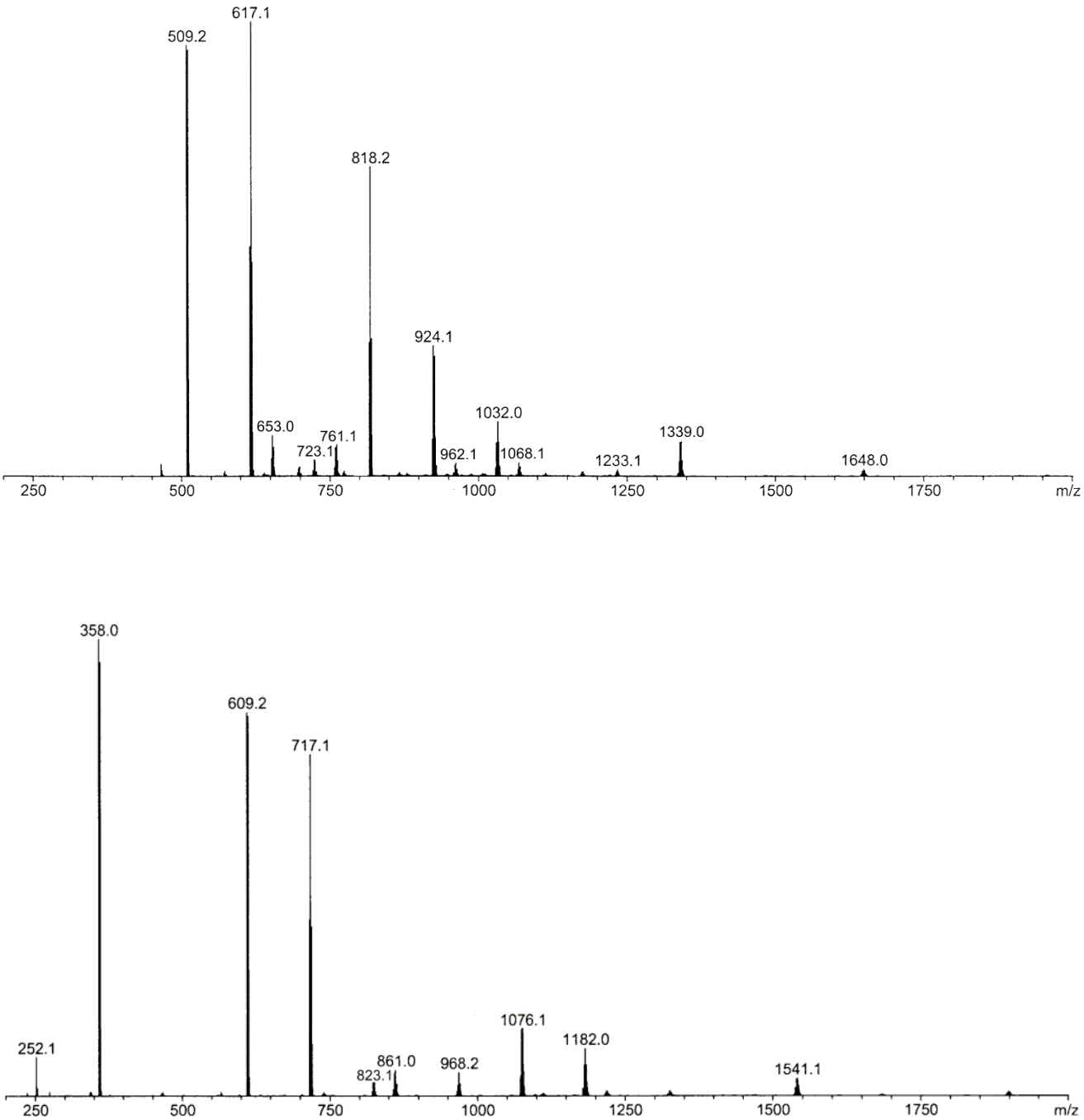

Fig S7 Electrospray mass spectra of **3** from MeCN solution (top), and of **4** from CH_2Cl_2 (bottom). See Table S7 for the peak assignments.

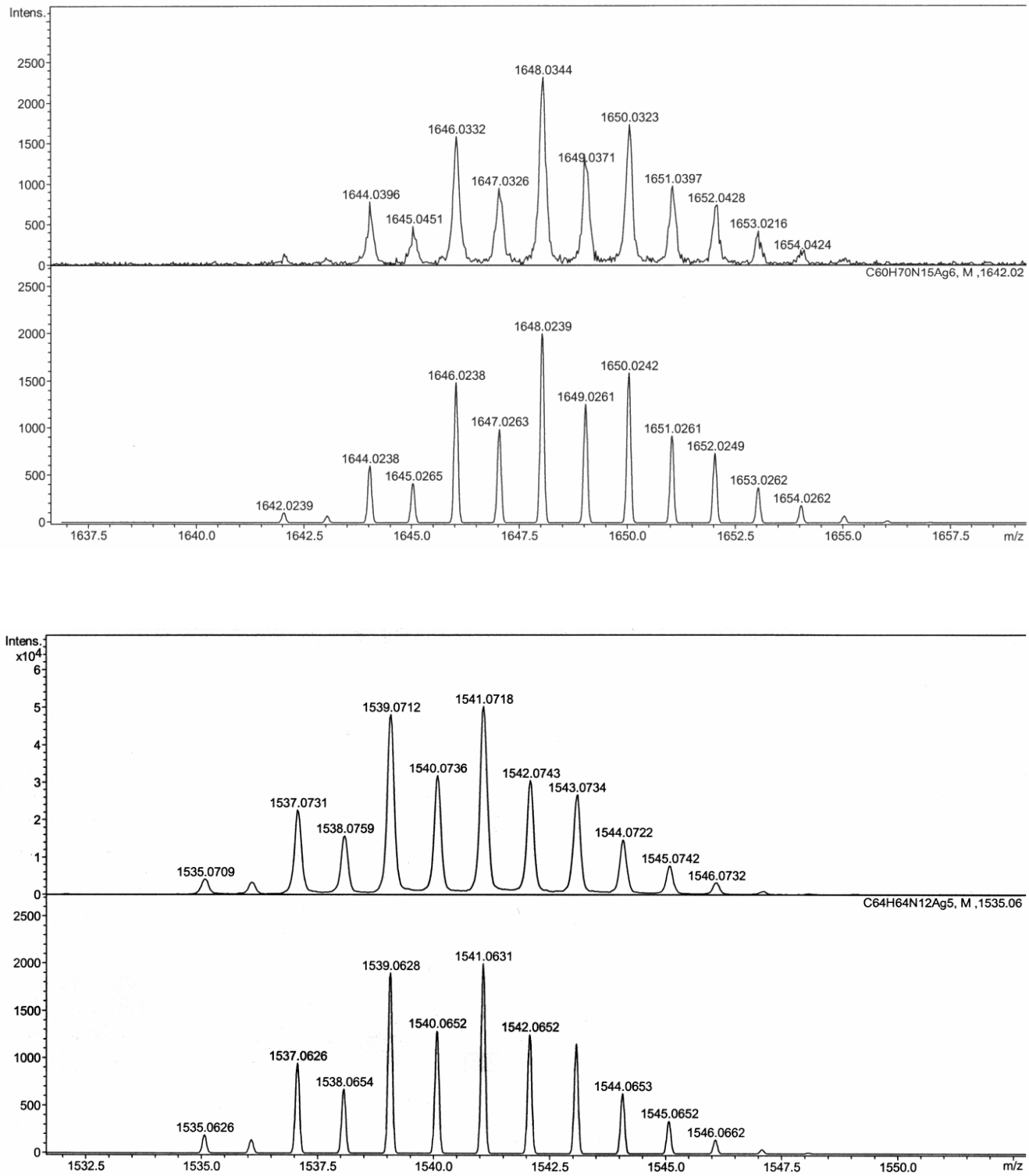

Fig S8 Representative observed and simulated mass peaks for the highest significant molecular ions in the mass spectra of **1**-**4** (Table S7): $[Ag_6(L^1)_5]^+$ in the spectrum of **3** (top), and $[Ag_5(L^2)_4]^+$ in the spectrum of **4** (bottom).

Table S7 Relative intensities and assignments of the peaks in the ES mass spectra of **1**-**4** from CH_2Cl_2 (**1**, **2** and **4**) or MeCN (**3**[a]; Figs. S6-S8). Only peaks with relative intensities >1 % relative to the most abundant molecular ion are listed. The proposed assignments are consistent with the isotopic patterns in each peak.

1-3					**4**		
m/z	Assignment	% in **1**	% in **2**	% in **3**[a]	*m/z*	Assignment	%
308.1	$[Ag(HL^1)]^+$	23	–	–	252.1	$[H_2L^2]^+$	8
509.2	$[Ag(HL^1)_2]^+$	97	100	93	358.0	$[Ag(HL^2)]^+$	100
617.1	$[Ag_2(L^1)(HL^1)]^+$	100	52	100	609.2	$[Ag(HL^2)_2]^+$	84
723.1	$[Ag_3(L^1)_2]^+$	15	–	5	717.1	$[Ag_2(L^2)(HL^2)]^+$	75
818.2	$[Ag_2(L^1)(HL^1)_2]^+$	–	29	68	823.1	$[Ag_3(L^2)_2]^+$	3
924.1	$[Ag_3(L^1)_2(HL^1)]^+$	18	12	29	861.0	$[Ag(L^2)(HL^2)_2]^+$	6
1032.0	$[Ag_4(L^1)_3]^+$	24	6	11	968.2	$[Ag_2(L^2)(HL^2)_2]^+$	5
1233.1	$[Ag_4(L^1)_3(HL^1)]^+$	–	–	2	1076.1	$[Ag_3(L^2)_2(HL^2)]^+$	15
1339.0	$[Ag_5(L^1)_4]^+$	13	3	7	1182.0	$[Ag_4(L^2)_3]^+$	10
1648.0	$[Ag_6(L^1)_5]^+$	3	–	2	1541.1	$[Ag_5(L^2)_4]^+$	4
653.0	$[Ag_2Cl(HL^1)_2]^+$	–	–	9			
761.1	$[Ag_3Cl(L^1)(HL^1)]^+$	–	–	8			
962.1	$[Ag_3Cl(L^1)(HL^1)_2]^+$	–	–	3			
1068.1	$[Ag_4Cl(L^1)_2(HL^1)]^+$	–	–	3			
697.0	$[Ag_2Br(HL^1)_2]^+$	–	9	–			
804.9	$[Ag_3Br(L^1)(HL^1)]^+$ ($[\mathbf{2}+H]^+$)	–	7	–			

[a]Solutions of **3** in MeCN, like the one used to acquire this mass spectrum, deposit an AgCl precipitate over a period of minutes. Hence, this spectrum may not be the true mass spectrum of **3** (MeCN was used in preference to CH_2Cl_2 for this compound because it leads to less rapid AgCl formation).

References

[1] W.-S. Yu, C.-C. Cheng, Y.-M. Cheng, P.-C. Wu, Y.-H. Song, Y. Chi and P.-T. Chou, *J. Am. Chem. Soc.*, 2003, **125**, 10800.
[2] S.-Y. Chang, J. Kavitha, S.-W. Li, C.-S. Hsu, Y. Chi, Y.-S. Yeh, P.-T. Chou, G.-H. Lee, A. J. Carty, Y.-T. Tao and C.-H. Chien, *Inorg. Chem.*, 2006, **45**, 137.
[3] G. M. Sheldrick, *Acta Cryst., Sect. A*, 2008, **64**, 112.
[4] L. J. Barbour, *J. Supramol. Chem.*, 2001, **1**, 189.
[5] *POVRAY* v. 3.5, Persistence of Vision Raytracer Pty. Ltd., Williamstown, Victoria, Australia, 2002.
[6] A. L. Spek, *J. Appl. Cryst.*, 2003, **36**, 7.
[7] K. Singh, J. R. Long and P. Stavropoulos, *J. Am. Chem. Soc.*, 1997, **119**, 2942.
[8] For other trinuclear silver(I) pyrazolides see *e.g.* H. H. Murray, R. G. Raptis and J. P. Fackler jr., *Inorg. Chem.*, 1988, **27**, 26; N. Masciocchi, M. Moret, P. Cairati, A. Sironi, G. A. Ardizzoia and G. La Monica, *J. Am. Chem. Soc.*, 1994, **116**, 7668; F. Meyer, A. Jacobi and L. Zsolnai, *Chem. Ber.*, 1997, **130**, 1441; S. Yamada, T. Ishida and T. Nogami, *Dalton Trans.*, 2004, 898; M. A. Omary, M. A. Rawashdeh-Omary, M. W. A. Gonser, O. Elbjeirami, T. Grimes, T. R. Cundari, H. V. K. Diyabalanage, C. S. P. Gamage, and H. V. R. Dias, *Inorg. Chem.*, 2005, **44**, 8200; A. A. Mohamed, L. M. Pérez and J. P. Fackler jr., *Inorg. Chim. Acta*, 2005, **358**, 1657; H. V. R. Dias and H. V. K. Diyabalanage, *Polyhedron*, 2006, **25**, 1655; J.-P. Zhang and S. Kitagawa, *J. Am. Chem. Soc.*, 2008, **130**, 907.
[9] K. Fujisawa, Y. Ishikawa, Y. Miyashita and K. Okamoto, *Inorg. Chim. Acta*, 2010, **363**, 2977.
[10] G. Yang and R. G. Raptis, *Inorg. Chim. Acta*, 2007, **360**, 2503.
[11] G. A. Ardizzoia, S. Cenini, G. La Monica, N. Masciocchi and M. Moret, *Inorg. Chem.*, 1994, **33**, 1458; K. Singh, J. R. Long and P. Stavropoulos, *Inorg. Chem.*, 1998, **37**, 1073; A. Maspero, S. Brenna, S. Galli and A. Penoni, *J. Organomet. Chem.*, 2003, **672**, 123; M. Stollenz, M. John, H. Gehring, S. Dechert, C. Grosse and F. Meyer, *Inorg. Chem.*, 2009, **48**, 10049.